2014

Behaviour of clay-fouled ballast under cyclic loading

Nayoma Tennakoon
University of Wollongong, nayoma@uow.edu.au

Buddhima Indraratna
University of Wollongong, indra@uow.edu.au

Publication Details

Tennakoon, N. & Indraratna, B. (2014). Behaviour of clay-fouled ballast under cyclic loading. Geotechnique: international journal of soil mechanics, 64 (6), 502-506.

Behaviour of clay-fouled ballast under cyclic loading

Abstract

Expansion of the rail network in congested coastal Australia compels track construction on soft clayey subgrade, including fine-grained estuarine soils. In such low-lying areas, where the water table is close to the ground surface, the saturated soft subgrade is often subjected to pumping (mud slurry) under the application of cyclic wheel loads, thereby causing fouling of the overlying ballast. This technical note presents the results of a series of large-scale, drained, cyclic, triaxial tests conducted on clay-fouled ballast. The impact of fouling on the stress-strain behaviour, resilient modulus and degradation of ballast is discussed.

Keywords

under, ballast, loading, fouled, cyclic, clay, behaviour

Disciplines

Engineering | Science and Technology Studies

Publication Details

Tennakoon, N. & Indraratna, B. (2014). Behaviour of clay-fouled ballast under cyclic loading. Geotechnique: international journal of soil mechanics, 64 (6), 502-506.

Tennakoon, N. & Indraratna, B. (2014). *Géotechnique* **64**, No. 6, 502–506 [http://dx.doi.org/10.1680/geot.13.T.033]

TECHNICAL NOTE

Behaviour of clay-fouled ballast under cyclic loading

N. TENNAKOON* and B. INDRARATNA*

Expansion of the rail network in congested coastal Australia compels track construction on soft clayey subgrade, including fine-grained estuarine soils. In such low-lying areas, where the water table is close to the ground surface, the saturated soft subgrade is often subjected to pumping (mud slurry) under the application of cyclic wheel loads, thereby causing fouling of the overlying ballast. This technical note presents the results of a series of large-scale, drained, cyclic, triaxial tests conducted on clay-fouled ballast. The impact of fouling on the stress–strain behaviour, resilient modulus and degradation of ballast is discussed.

KEYWORDS: clays; deformation; gravels; laboratory tests

INTRODUCTION

To ensure the longevity and serviceability of rail tracks, it is essential to maintain ballast in a relatively fresh or uncontaminated state (Selig & Waters, 1994; Indraratna *et al.*, 2011). However, with time, ballast becomes fouled due to: (*a*) breakage of angular corners and sharp edges; (*b*) infiltration of fines from the surface; and (*c*) subgrade soil pumping under excessive cyclic loads when saturated (Feldman & Nissen, 2002; Indraratna *et al.*, 2013). To quantify ballast fouling, the void contaminant index (VCI), defined as the ratio of the bulk volume of fouling material to the volume of voids in clean ballast (Tennakoon *et al.*, 2012), is now adopted widely by rail organisations in the state of New South Wales.

In the past, there have been several studies conducted on the triaxial behaviour of ballast (Indraratna *et al.*, 1998; Suiker *et al.*, 2005; Anderson & Fair, 2008; Aursudkij *et al.*, 2009; Sevi *et al.*, 2009). However, there has only been limited research carried out on the behaviour of clay-fouled ballast (Huang *et al.*, 2009; Indraratna *et al.*, 2013). Indraratna *et al.* (2013) conducted monotonic loading tests on clay-fouled ballast and showed that fouling reduced the effective angularity of the ballast, and decreased its overall shear strength. At significantly higher levels of fouling by clay, the ballast specimens showed an increasingly ductile behaviour. It was also postulated that fouled ballast would become less compressive as the voids become increasingly filled, while the binding effect introduced by the cohesive clay would reduce the tendency of the aggregates to dilate readily. In this technical note, the above research conducted under monotonic loading has been extended further by a series of large-scale, cyclic, triaxial tests conducted at a frequency of 20 Hz, representing 25 t axle trains operating at speeds in the vicinity of 150 km/h.

Manuscript received 25 November 2013; revised manuscript accepted 11 March 2014. Published online ahead of print 20 May 2014.
Discussion on this paper closes on 1 November 2014, for further details see p. ii.
* Centre for Geomechanics and Railway Engineering, Faculty of Engineering and Information Sciences, University of Wollongong, Wollongong City, NSW, Australia

EXPERIMENTAL PROCEDURE

A series of large-scale triaxial tests at a confining pressure of 10 kPa was conducted under different magnitudes of fouling (VCI = 0, 10, 25, 50 and 80%). It has been clarified in earlier studies that a sample size ratio (i.e. diameter of the test specimen to the maximum particle size of the testing material) of at least 6 would ensure that the sample size effects would not adversely influence the rockfill properties (Marachi *et al.*, 1972; Indraratna *et al.*, 1993, 2013). In this study, a large-scale triaxial apparatus that could accommodate a specimen 600 mm high and 300 mm in diameter was used. The gradation curves for ballast and clay are shown in Fig. 1. The maximum grain size fraction (d_{95}) was less than 50 mm, thereby resulting in a sample size ratio of 6. For the finest particle size fraction ($d_{10} < 30$ mm), the size ratio exceeds 10. These size ratios ensure that the influence of size effects on the triaxial properties of ballast is insignificant. Commercial kaolin clay was used to represent the contaminated fines in the ballast (i.e. fouling material).

Under normal track environments, there is significant lateral movement observed in the ballast layer due to the reduced lateral restraint at the edge of sleeper (Lackenby *et al.*, 2007; Indraratna *et al.*, 2010a, 2011). Therefore, only a small confining pressure ($\sigma_3 = 10$ kPa) was applied to the triaxial specimens to represent realistic field conditions. More details on the experimental procedure, material and

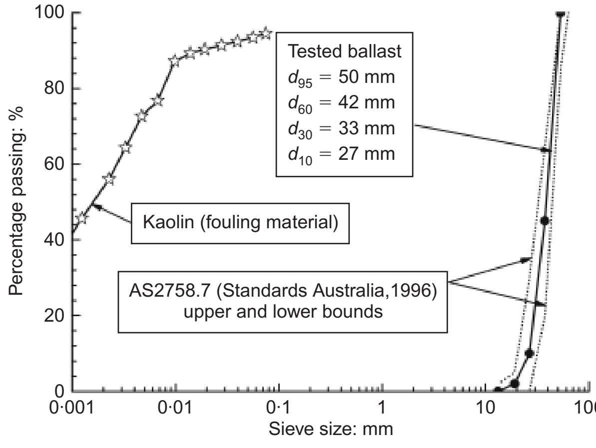

Fig. 1. Particle size distribution of test materials

specimen preparation are explained elsewhere (Indraratna *et al.*, 2013).

For most operating conditions on long, flat tracks, the major principal stress is vertical (due to heavy axle load), and the relatively small minor principal stress is the lateral confining pressure provided by the sleepers and ballast assembly. At significant acceleration/deceleration, some principal stress rotation would occur even on flat tracks. The rotation of principal stresses may generate larger plastic deformations (Gräbe & Clayton, 2009) and result in a reduced resilient modulus (Wong & Arthur, 1986). Nevertheless, the conventional triaxial testing is still sufficient to simulate the in-situ track conditions for most operational scenarios, except at significant train acceleration.

The cyclic stress was varied between the maximum deviator stress (q_{max}) and the minimum deviator stress (q_{min}). The value of q_{min} was set to 45 kPa, which represents the lowest point on the cyclic loading–unloading curve following q_{max} of 230 kPa (for a typical axle load of 25 t), incorporating a track confining pressure of 10 kPa (Salim, 2004; Lackenby *et al.*, 2007). These cyclic loading and unloading values have been measured in fully instrumented tracks located in the towns of Bulli, Singleton and Sandgate (Indraratna *et al.*, 2010a, 2010b, 2014), and the corresponding confining pressure in the vicinity of 10 kPa has been established as realistic for typical conditions of ballast–sleeper assembly installed in tracks in Australia. The value of q_{max} was set equal to 230 kPa, representing a typical 25 t axle load (Lackenby *et al.*, 2007). Fig. 2 shows the details of the cyclic loading applied during the testing programme.

A loading frequency of 20 Hz was used to simulate a typical train speed of approximately 150 km/h, assuming an axle wheel spacing of 2·02 m. If the resonant frequency is reached, the settlement would increase rapidly and become greater than the maximum settlement under the corresponding mean static load (Terzaghi *et al.*, 1996). However, the comparison with static test results from Indraratna *et al.* (2013) indicated that the resonant frequency did not reach to the proximity of 20 Hz. Permanent deformations were recorded at regular intervals, while bursts of data (sampling frequency = 590 Hz) were recorded at specific cycles to determine the resilient modulus. Testing was continued for 500 000 cycles or until an axial strain of 28% was reached (i.e. the limit of the actuator displacement). Sieving was carried out at the completion of each test and compared with the original particle size distribution to evaluate the extent of breakage.

RESULTS AND DISCUSSION

Development of strain and pore pressure

Figure 3(a) illustrates the variation in axial strain of fouled ballast (VCI up to 80%) compared to clean ballast

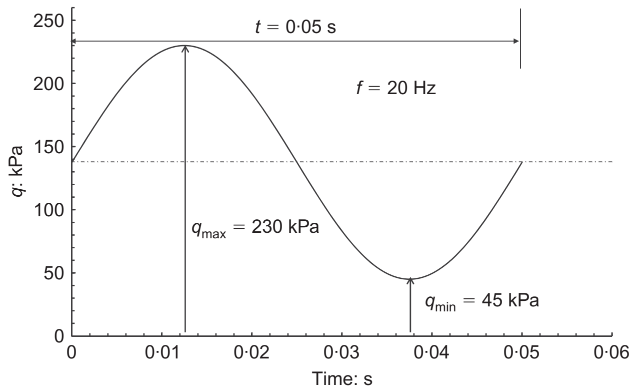

Fig. 2. Cyclic stress configuration

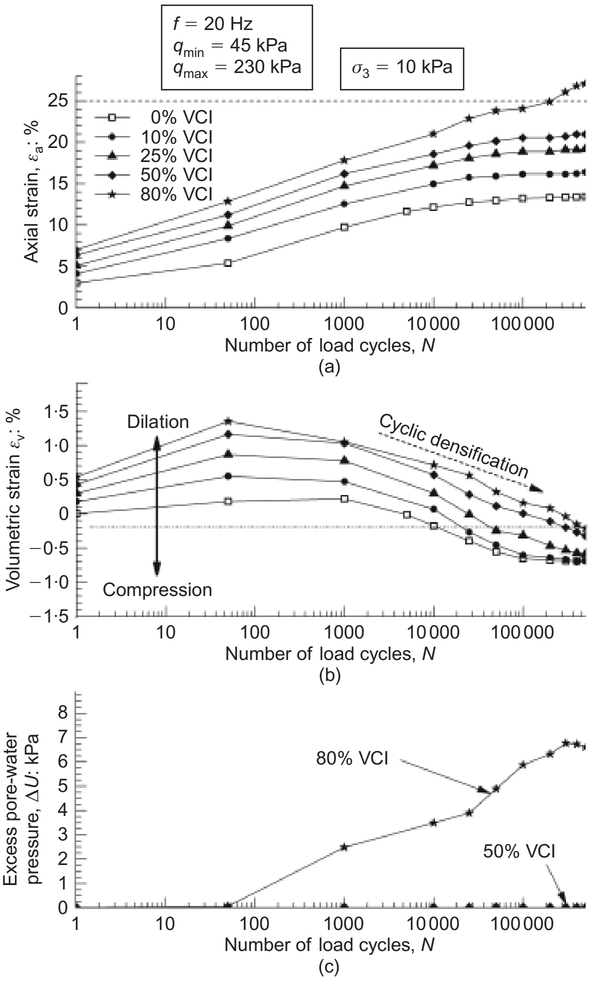

Fig. 3. Strain response under cyclic loading: (a) axial strain, ε_a; (b) volumetric strain, ε_v; (c) excess pore-water pressure measured at the middle of the specimen, as a function of the number of load cycles, N

(VCI = 0%) with the number of load cycles (N) at an initial confining pressure (σ_3) of 10 kPa. For VCI between 0% and 50%, the axial strains gradually increased at a decreasing rate as N increased up to 50 000 cycles, thereafter approaching a constant value. However, for VCI = 80%, the axial strain continued to increase (i.e. without attaining a stable level) for $N > 100\,000$ cycles. For high levels of fouling (VCI = 80%), the axial strains > 25% at $N = 200\,000$ can be considered as approaching failure of the specimen, in comparison with the more stable axial strain observed for the other specimens (VCI ⩽ 50%). The test conditions were deliberately extended to capture the worst possible scenario with axial strain exceeding 20% (i.e. until the limit of the axial loading actuator was reached). These ‘severe conditions’ are not uncommon in situations where the fouling material (clay) ‘lubricates’ the otherwise rough surface texture of highly angular ballast, thereby facilitating significantly larger axial strains. In order to simulate badly affected tracks due to subgrade pumping, especially in tracks constructed over low-lying estuarine terrains, large deformation tests of clay-fouled ballast represent realistic practical situations.

Figure 3(b) shows the changes in volumetric strain with respect to N, for varying levels of fouling at σ_3 of 10 kPa. It was observed that the fouled ballast specimens dilated initially and this was then followed by compression, as subsequent densification occurred with the increasing number of cycles. With the increase of VCI, the corresponding maximum dilation also increased, and this may be attributed to the reduction in the overall porosity as clay now occupies a substantial portion of the voids between aggregates and thereby impedes particle densification (compression) under cyclic loading. In contrast to fouled ballast, fresh ballast showed only a slight dilation for $N < 1000$, but indicated considerable compression or progressive densification at higher loading cycles.

Figure 3(c) shows the development of excess pore-water pressure for VCI = 80%, with the increasing number of cycles. Clearly, this build-up of excess pore-water pressure was caused by the application of a relatively high frequency ($f = 20$ Hz) that had not allowed sufficient time for the excess pore pressure to dissipate. Not surprisingly, at the initial phase ($N \leqslant 50$) where the specimen exhibited a dilative response (Fig. 3(b)), no excess pore-water pressure was recorded. However, as expected, when the specimen was subjected to cyclic densification at larger values of N, the excess pore-water pressure gradually increased.

Figure 4 illustrates the final (accumulated) axial strains of all specimens as a function of the VCI for $N = 500\,000$. Up to VCI = 50%, the final axial strains gradually increased, but at a declining rate. However, for high level of fouling (VCI = 80%), the final axial strain increased at a much higher rate than the other specimens of lower VCI. Although the number of test data is limited, based on these observations, three distinct zones (Fig. 4) could be identified.

1. Zone 1 (lubrication effect): for VCI ⩽ 25%, this zone of increasing final axial strains could be attributed to the infilled clay forming a thin coating over the rock aggregates, thereby providing a 'lubrication' effect, reducing the inter-particle friction. In this zone, the clay content is not sufficient to impede 'free-draining' of ballast.
2. Zone 2 (stabilisation effect): for 25% < VCI ⩽ 50%, the final strains seem to increase only marginally, indicating a 'stabilisation' effect. In this zone, sufficient drainage still occurs within the clay-fouled granular assembly.
3. Zone 3 (impeded drainage): for VCI > 50%, the excessive clay content in the ballast starts to impede drainage. The behaviour is now predominantly governed by the clay matrix, generating excess pore-water pressure with the increasing number of cycles.

Resilient modulus, M_r

Under cyclic loading, the resilient modulus (M_r) of ballast is a very important factor in track substructure design and performance evaluation, apart from characterising the specimen stiffness and the corresponding axial deformation (Ozel & Mohajerani, 2001; Lackenby *et al.*, 2007). Excessive ballast deformation contributes to reduced track longevity, while differential track settlements often affect speed restrictions (Arangie & Maree, 1999). The resilient modulus M_r is calculated using equation (1), where $\Delta_{q,\mathrm{cyc}}$ is the magnitude of deviator stress ($q_{\max} - q_{\min}$), and $\varepsilon_{\mathrm{a,rec}}$ is the recoverable portion of the axial strain.

$$M_r = \frac{\Delta_{q,\mathrm{cyc}}}{\varepsilon_{\mathrm{a,rec}}} \tag{1}$$

Figure 5 shows the resilient modulus (M_r) as a function of N for different degrees of fouling. M_r increased with an increase of N at a diminishing rate towards a stable value under cyclic densification. For VCI > 25%, a constant volumetric strain is reached after $N > 100\,000$. Fig. 5 verifies that an increased level of fouling leads to a considerable decrease in M_r (i.e. about 40% drop from fresh ballast when VCI = 80%). The reduced magnitude of M_r of clay-fouled ballast implies the occurrence of higher axial strain compared to that of clean ballast for a given number of cycles.

Ballast breakage

In this study, the ballast breakage index (BBI) introduced by Indraratna *et al.* (2005) was taken to quantify the breakage of aggregates under cyclic loading. In this approach, by plotting the particle size distribution (PSD) before and after testing, the extent of breakage can be quantified with reference to an arbitrary boundary for a well-graded sand considered as the lower limit of the ballast PSD, if breakage is allowed to continue. When clay intrudes the ballast voids (fouling), the rate and magnitude of breakage is expected to alter for the same loading conditions.

Figure 6 shows the BBI as a function of VCI, which confirms that the aggregates experience less breakage at higher values of VCI. This is not surprising, because the increased clay content would provide adequate 'cushioning' to prevent the harsh attrition between the rough and angular ballast grains; that is, reducing the stress concentrations that cause rapid splitting at the particle corners.

CONCLUSIONS

The behaviour of clay-fouled ballast under cyclic loading was studied, and the following salient conclusions could be drawn.

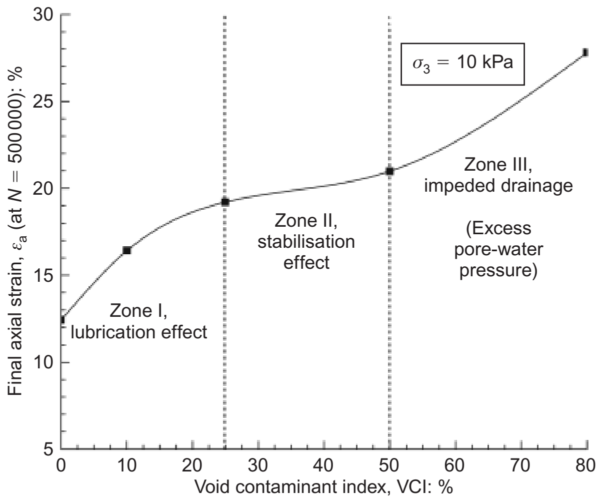

Fig. 4. Final axial strain ε_a at 500 000 cycles as a function of the VCI

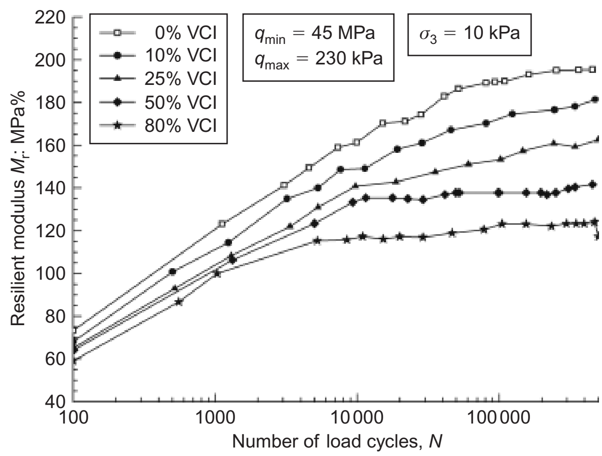

Fig. 5. Variation of resilient modulus, M_r, as a function of number of load cycles, N

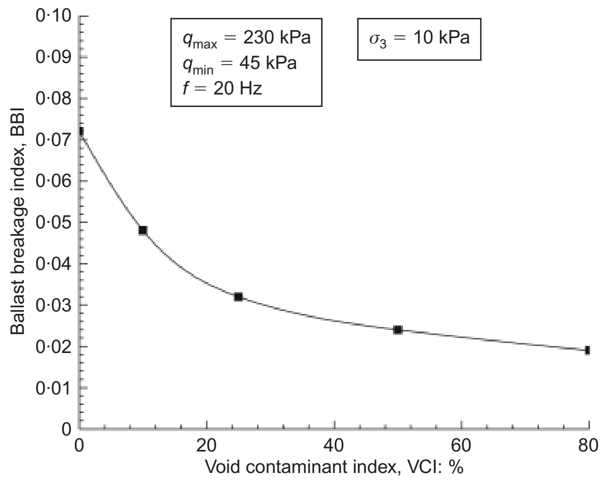

Fig. 6. Ballast breakage index (BBI) as a function of VCI

(*a*) In general, the axial and volumetric strains increased with the degree of fouling or VCI, at any given number of loading cycles, *N*.
(*b*) In particular, the increased degree of fouling from zero (fresh ballast) to VCI = 80% was accompanied by an increase in maximum volumetric dilation for $N < 100$, and a reduction in the final compressive strain for $N > 1000$.
(*c*) For high levels of fouling by clay (VCI = 80%), the ballast specimens tested at a relatively high frequency of 20 Hz experienced a build-up of excess pore-water pressure for $N > 50$, when natural 'free draining' was impeded within the granular assembly.
(*d*) Depending on the extent of clay fouling or the magnitude of VCI, the increasing trend of final axial strains demarcated three separate zones, representing:
   (i) lubrication effect for low levels of fouling, VCI < 25%
   (ii) stabilisation effect for intermediate fouling (25% < VCI < 50%)
   (iii) impeded drainage when VCI significantly exceeded 50%.
(*e*) As VCI increased, the particle breakage was observed to decrease. This may be attributed to the 'cushioning' effect provided by the clay seam between the angular aggregates, partially protecting them against harsh abrasion.

ACKNOWLEDGEMENTS

The authors acknowledge the ARC Centre of Excellence in Geotechnical Science and Engineering and the CRC for Rail Innovation for their support. The assistance of Assistant Professor Cholachat Rujikiatkamjorn, Dr Sanjay Nimbalkar and Mr Andrew Howle at various stages of this research is appreciated.

NOTATION

d_{10} grain diameter at 10% passing
d_{95} grain diameter at 95% passing
f loading frequency
M_r resilient modulus (MPa)
N number of cycles
q_{max} maximum deviator stress (kPa)
q_{min} minimum deviator stress (kPa)
t time (s)
ΔU excess pore-water pressure (kPa)
$\Delta_{q,cyc}$ $q_{max} - q_{min}$ (kPa)
ε_a axial strain (%)
$\varepsilon_{a,rec}$ recoverable portion of the axial strain
ε_v volumetric strain (%)
σ_3 confining pressure (kPa)

REFERENCES

Anderson, W. & Fair, P. (2008). Behavior of railroad ballast under monotonic and cyclic loading. *J. Geotech. Geoenviron. Engng ASCE* **134**, No. 3, 316–327.

Arangie, P. B. D. & Maree, L. (1999). Predicting the resilient behaviour of railway ballast. *J. South African Instn Civ. Engng* **41**, No. 1, 21–25.

Aursudkij, B., McDowell, G. R. & Collop, A. C. (2009). Cyclic loading of railway ballast under triaxial conditions and in a railway test facility. *Granular Matter* **11**, No. 6, 391–401.

Feldman, F. & Nissen, D. (2002). Alternative testing method for the measurement of ballast fouling: percentage void contamination. *Conference on railway engineering RTSA*, Wollongong, NSW, pp. 101–111. Canberra, Australia: Railway Technical Society of Australasia.

Gräbe, P. J. & Clayton, C. R. (2009). Effects of principal stress rotation on permanent deformation in rail track foundations. *J. Geotech. Geoenviron. Engng, ASCE* **135**, No. 4, 555–565.

Huang, H., Tutumluer, E. & Dombrow, W. (2009). Laboratory characterization of fouled railroad ballast behavior. *Transport Res. Record: J. Transport Res. Board* **2117**, 93–101.

Indraratna, B., Wijewardena, L. S. S. & Balasubramaniam, A. S. (1993). Large-scale triaxial testing of greywacke rockfill. *Géotechnique* **43**, No. 1, 37–51, http://dx.doi.org/10.1680/geot.1993.43.1.37.

Indraratna, B., Ionescu, D. & Christie, D. (1998). Shear behaviour of rail ballast on large scale triaxial testing. *J. Geotech. Geoenviron. Engng ASCE* **124**, No. 5, 439–449.

Indraratna, B., Lackenby, J. & Christie, D. (2005). Effect of confining pressure on the gradation of ballast under cyclic loading. *Géotechnique* **55**, No. 4, 325–328, http://dx.doi.org/10.1680/geot.2005.55.4.325.

Indraratna, B., Nimbalkar, S., Christie, D., Rujikiatkamjorn, C. & Vinod, J. S. (2010a). Field assessment of the performance of a ballasted rail track with and without geosynthetics. *J. Geotech. Geoenviron. Engng ASCE* **136**, No. 7, 907–917.

Indraratna, B., Rujikiatkamjorn, C., Adams, M. & Ewers, B. (2010b). Class A prediction of the behaviour of soft estuarine soil foundation stabilised by short vertical drains beneath a rail track. *Int. J. Geotech. Geoenviron. Engng ASCE* **136**, No. 5, 686–696.

Indraratna, B., Salim, W. & Rujikiatkamjorn, C. (2011). *Advanced rail geotechnology – ballasted track*. Boca Raton, Florida, USA: CRC Press; Leiden, the Netherlands: Balkema.

Indraratna, B., Tennakoon, N., Nimbalkar, S. & Rujikiatkamjorn, C. (2013). Behaviour of clay fouled ballast under drained triaxial testing. *Géotechnique* **63**, No. 5, 410–419, http://dx.doi.org/10.1680/geot.11.P.086.

Indraratna, B., Nimbalkar, S. & Neville, T. (2014). Performance assessment of reinforced ballasted rail track. *Proc. Instn Civ. Engrs Ground Improvement* **167**, No. 1, 24–34.

Lackenby, J., Indraratna, B., McDowell, G. R. & Christie, D. (2007). Effect of confining pressure on ballast degradation and deformation under cyclic triaxial loading. *Géotechnique* **57**, No. 6, 527–536, http://dx.doi.org/10.1680/geot.2007.57.6.527.

Marachi, N. D., Chan, C. K. & Seed, H. B. (1972). Evaluation of properties of rockfill materials. *J. Soil Mech. Found. Div. ASCE* **98**, No. SM1, 95–114.

Ozel, M. R. & Mohajerani, A. (2001). Resilient modulus of a stabilised fine grained subgrade soil. *Australian Geomechanics* **36**, No. 3, 75–86.

Salim, M. W. (2004). *Deformation and degradation aspects of ballast and constitutive modelling under cyclic loading*. PhD thesis, University of Wollongong, Australia.

Selig, E. T. & Waters, J. M. (1994). *Track technology and substructure management*. London, UK: Thomas Telford.

Sevi, A. F., Ge, L. & Take, W. A. (2009). A large-scale triaxial apparatus for prototype railroad ballast testing. *Geotech. Testing J.* **32**, No. 4, paper 102033.

Standards Australia (1996). *AS 2758.7 – Part 7. Aggregates and* *rock for engineering purposes – railway ballast*. Sydney, NSW, Australia: Standards Australia.

Suiker, A. S. J., Selig, E. T. & Frenkel, R. (2005). Static and cyclic triaxial testing of ballast and subballast. *J. Geotech. Geoenviron. Engng ASCE* **131**, No. 6, 771–782.

Tennakoon, N., Indraratna, B., Rujikiatkamjorn, C., Nimbalkar, S. & Neville, T. (2012). The role of ballast-fouling characteristics on the drainage capacity of a rail substructure. *Geotech. Testing J.* **35**, No. 4, 1–12.

Terzaghi, K., Peck, R. B. & Mesri, G. (1996). *Soil mechanics in engineering practice*. New York, NY, USA: Wiley.

Wong, R. K. S. & Arthur, J. R. F. (1986). Sand sheared by stresses with cyclic variations in direction. *Géotechnique* **36**, No. 2, 215–226, http://dx.doi.org/10.1680/geot.1986.36.2.215.